

Electronic Supplementary Information for

## Transient Reshaping of Intraband Transitions by Hot Electrons

Benjamin T. Diroll<sup>\*a</sup> and Tathagata Banerjee<sup>a,b</sup>

\*bdiroll@anl.gov

<sup>a</sup>Center for Nanoscale Materials, Argonne National Laboratory

<sup>b</sup>Department of Physics, University of Illinois Urbana-Champaign

### Materials and Methods

**Materials.** Cadmium acetate hydrate ( $\geq 99.99\%$ , Aldrich), cadmium chloride (99.99%, Aldrich), selenium (99.99 %, powder,  $\sim 100$  mesh, Aldrich), 1-octadecene (90 %, technical grade, Aldrich), oleic acid (90 %, technical grade, Aldrich), cadmium nitrate (97 %, Aldrich), and sodium myristate ( $>98\%$ , Aldrich) were sourced from commercial suppliers and used as received. Solvents used were sourced from commercial suppliers and were ACS grade or higher.

**Synthesis.** Cadmium myristate was synthesized by dissolving 1.5 g sodium myristate in methanol (via sonication) and then adding 600 mg of cadmium nitrate under stirring. The methanolic solution immediately becomes cloudy and is then stirred under air for 4 hours, then the white solid was isolated by centrifugation at 5000 rpm. The white precipitate was re-dispersed in methanol and precipitated two more times, then once using acetone. Cadmium myristate was isolated as a white powder after vacuum drying for 16 hours at 60 °C. 4.5 ML CQWs were synthesized by combining 12 mg Se powder, 170 mg cadmium myristate, and 15 mL octadecene, which are held under vacuum at room temperature for 1 hour, then heated under nitrogen to 240 °C. At 195 °C, under nitrogen counterflow, 40 mg of finely-ground cadmium acetate was added rapidly. After 5 minutes at 240 °C, the reaction was cooled by removing the heating mantle and 2 mL of oleic acid was injected, followed at  $\sim 100$  °C with 10 mL of toluene. NPLs were precipitated from the reaction medium by centrifugation at 15000 rpm, then re-dispersed into methylcyclohexane. 5.5 ML CQWs were synthesized by mixing 170 mg cadmium myristate in 14 mL octadecene, holding under vacuum for 1 hour at room temperature, then heated under nitrogen to 250 °C. At 250 °C, a dispersion of 12 mg selenium in 1 mL octadecene (dispersed with sonication and vigorous mixing) was rapidly injected, followed, after 1 minute, by addition of 90 mg cadmium acetate with nitrogen counterflow. The reaction proceeded for an additional 15 minutes. After removal of the heating mantle, 2 mL of oleic acid was injected, followed at 100 °C with 10 mL of toluene. Samples were isolated by centrifugation of the reaction mixture at 15000 rpm, with the sample re-dispersed and stored in methylcyclohexane. 6.5 ML CQWs were prepared by mixing 170 mg cadmium myristate and 14 mL octadecene, held under vacuum for 30 minutes at 85 °C, then heating under nitrogen to 250 °C. At 250 °C, a dispersion of 12 mg selenium in 1 mL octadecene (dispersed with sonication and vigorous mixing) was rapidly injected, followed, after 20 seconds, by addition of 60 mg cadmium myristate with nitrogen counterflow. The reaction proceeded for an addition 60 seconds, then a dropwise injection of 0.15 mL 0.5 M cadmium chloride in water over two minutes. After an additional 3 minutes, the reaction was cooled by removing the heating mantle. At 150 °C, 2 mL oleic acid and 15 mL methylcyclohexane was injected. The reaction medium was centrifuged to precipitate a mixture which contains 6.5 ML NPLs, thinner NPLs, and other small particles, which were separated by size-selective precipitation of methylcyclohexane dispersions.

**Transmission Electron Microscopy (TEM).** Transmission electron microscopy characterization was performed using a JEOL-2100F.

**Static Spectroscopy.** Absorption spectra were collected using a Cary-50 spectrophotometer.

**Time-Resolved Spectroscopy.** Ultrafast pump-probe transient absorption and related pump-push-probe experiments were performed by splitting the fundamental output of a 2 kHz 1.55 eV

Ti:sapphire laser. One branch chopped to 1 kHz is the pump branch and converted either by frequency-doubling or using an optical parametric amplifier (OPA) to an energy of choice. The second branch was focused into a 5mm sapphire crystal to generate a supercontinuum white light probe in the near-infrared. Pump and probe branches were spatially overlapped at the sample and Pump and probe delay were controlled using an optical delay stage. For Pump-push-probe experiments, the pump branch was additionally split into two, with one path frequency doubled to 3.10 eV and chopped to 1 kHz forming the pump; the other branch was directed through an OPA to generate mid-infrared light varying from 0.46 eV to 0.20 eV to become the push pulse. The probe was generated in the same as pump-probe experiments. Pump, push, and probe were spatially overlapped at the sample position. The pump-push delay was set to 14 ps by a separate delay stage.

*Fitting procedure.* The first to second intersubband absorption may be described using a Lorentzian (L) line-shape and the occupations of the upper and lower sub-bands:

$$\alpha(E) \propto \int d^2k_{\perp} f(E_1^s)(1 - f(E_2^s))L(E_2^s - E_1^s - E)$$

in which  $f$  is the Fermi-Dirac distribution and  $E_1^s$  and  $E_2^s$  give the dispersion of the respective first and second conduction bands.<sup>1</sup> This formulation is akin to descriptions of the band gap absorption or emission used to describe absorption or spontaneous and stimulated emission rates, but the coordinate of energy is distinct.<sup>2</sup> The energy coordinate which is used in the main text may be obtained from a simple description of the joint optical density of states. Generically, for an interband absorption, for which  $E_1$  is the valence band and  $E_2$  the conduction band,

$$E_1 = E_{1_0} - \frac{\hbar^2 k^2}{2m_1} \quad \text{and} \quad E_2 = E_{2_0} + \frac{\hbar^2 k^2}{2m_2}$$

to yield a joint optical density of states from the band gap ( $E_g$ ) and reduced mass of effective masses ( $m_r$ ):

$$(\pi\hbar^2)^{-1}(2m_r)^{3/2}(E - E_g)^{1/2}$$

For the intersubband transition, the first ( $E_1$ ) and second energy subbands ( $E_2$ ) are

$$E_1 = E_{1_0} + \frac{\hbar^2 k^2}{2m_1} \quad \text{and} \quad E_2 = E_{2_0} + \frac{\hbar^2 k^2}{2m_2}$$

To yield a joint optical density of states from the intersubband gap ( $E_g$ ):

$$(\pi\hbar^2)^{-1}(2m_r)^{3/2}(E_g - E)^{1/2}$$

One reasonable estimation of the effective mass for cadmium selenide at the band edge and the higher second subband can be obtained from works which have performed effective mass modelling. In these works, which have been able to reproduce the quasiparticle gaps of CdSe CQWs with reasonable accuracy, the effective mass as a function of energy is:

$$m_e(E) = \left( \alpha + \frac{E_p}{3} \left( \frac{2}{E + E_g} + \frac{1}{E + E_g + \Delta} \right) \right)^{-1}$$

In which  $E_g$  is the bulk band gap (here using 1.66 eV),  $E_p$  is Kane energy (16.5 eV),  $\Delta$  is spin-orbit splitting of the valence band (0.39 eV), and  $\alpha$  describes coupling of electrons to higher bands (-1.54 eV),<sup>3,4</sup> which may be graphically describes as in Figure S1.

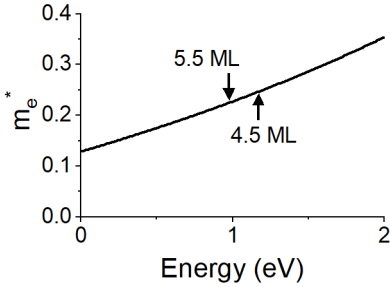


Figure S1. Energy-dependent effective electron mass of CdSe with arrows indicating the values of the  $E_2$  second electron subband positions of 4.5 ML and 5.5 ML CdSe CQWs.

For the band edge, the effective mass is  $m_1=0.13$ ; using this model, the effective mass of the second condition band in 5.5 monolayer CdSe CQWs is 0.22 and for 4.5 monolayer CQWs the value is 0.25, based upon the energy of the intersubband transitions above the band edge. Thus, the relevant reduced masses for the joint optical density of states are 0.082 and 0.085 for the 4.5 and 5.5 monolayer samples, respectively. For reference, the relevant reduced mass for interband transitions in CdSe is 0.1 (larger joint optical density of states), based upon a hole effective mass of 0.53; for gallium arsenide, c. 0.06 (smaller joint optical density of states); for methylammonium lead trihalide the reduced mass is 0.128. The value of reduced mass for the intersubband transitions of the CQWs falls between those of interband transitions of semiconductors to which the Boltzman hot carrier approximation has previously been applied.<sup>5-7</sup>

Simplification by removal of  $k$  selection rules still permits  $T_e$  estimation, which is more simply achieved using a Boltzman distribution as described in the text.<sup>8-11</sup> Previous investigations of, initially, gain spectra,<sup>12</sup> and subsequently hot electron behavior<sup>9,13-16</sup> of interband transitions have demonstrated that experimentally observed spectroscopic results cannot be obtained under strict  $k$ -selection rules with the joint optical density of states. In fact, momentum conservation is likely preserved through multiple excitation of electrons and holes,<sup>12</sup> similar to previously known processes in highly defective materials.<sup>17</sup> Subsequently, this was also found for intersubband transitions in several works. In particular, it was found that violate of  $k$ -selection via surface phonons and LO phonons is critical to explain non-inversion gain and tail absorption.<sup>18-22</sup> In addition to these observations, the CQWs themselves are also anticipated to display relaxation of  $k$ -selection due to their thin two-dimensionality,<sup>23,24</sup> defects such as surfaces,<sup>17</sup> or spatially localized excitons,<sup>25</sup> as for example predicted from gain<sup>26</sup> and optical stark effect measurements of CQWs.<sup>27</sup>

As shown in Figure 3, a range of experimental data from c. 75 meV from the intersubband peak extinction (at long delay times) was fit to obtain an estimated temperature. A sensitivity analysis was performed to determine the range of datapoints to fit and their influence on the net results. The fitted temperatures reported in this work are results which were insensitive to marginally expanding or reducing the fitted data range.

*Heating estimates based upon electron heat capacity.* If the electron heat capacity of CdSe is known, then the temperature of excited electrons may estimated from the excess pump photon energy. In this case, there is no data on the electronic heat capacity of CdSe CQWs, but there is at least some limited data on CdSe nanocrystals which permits an estimate of  $C_e = \gamma T$  under an approximation, where  $\gamma \approx 1.1 \times 10^{-2}$  J·mol<sup>-1</sup>·K<sup>-1</sup> based upon extrapolation of available experimental data to a diameter value corresponding to the thickness of the 4.5 monolayer CQWs (about half of the smallest quantum dot measured).<sup>28</sup> This may in turn be converted to a specific heat per electron as a function of temperature, shown in Figure S#. The excess energy available to electrons may be estimated based upon the photon energy of the pump and

the effective masses as  $\Delta E_e = \Delta E / (1 + m_e/m_h)$ .<sup>29</sup> By integrating the temperature-dependent electron heat capacity up to the value of  $\Delta E_e$ , we obtain an estimated final temperature after photoexcitation of c. 3400 K. This finding is not entirely consistent with our work in that the trend to smaller electronic heat capacities with larger sizes reported in literature indicates that the 5.5 monolayer sample would be expected to have higher, not lower, effective temperatures (c. 4000 K under the same approximations with  $\gamma \approx 0.8 \times 10^{-2} \text{ J}\cdot\text{mol}^{-1}\cdot\text{K}^{-1}$ ).

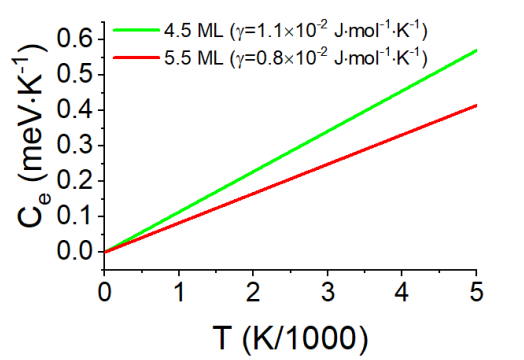


Figure S2. Electron heat capacities of 4.5 ML and 5.5 ML CdSe CQWs estimate from literature values of  $\gamma$ .

### Supplementary Data and Figures

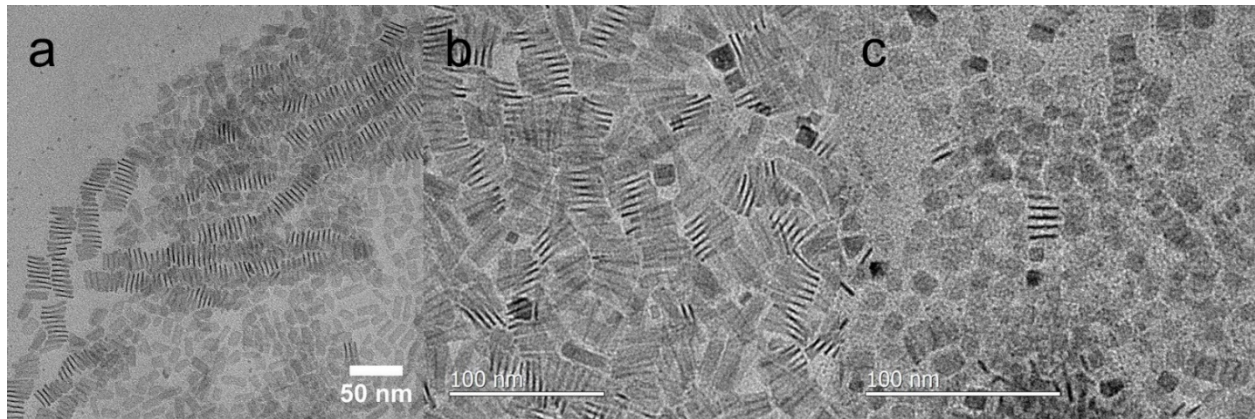


Figure S3. Transmission electron microscopy (TEM) images of (a) 4.5 ML, (b) 5.5 ML, and (c) 6.5 ML CdSe CQW samples.

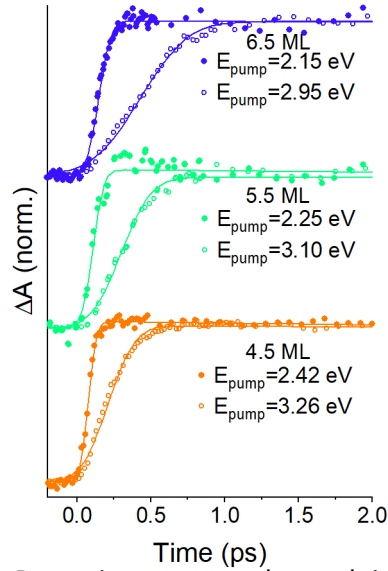


Figure S4. Dynamics traces at the peak intersubband absorption energy for the first two picoseconds of pump-probe delay for 4.5, 5.5, and 6.5 ML CdSe CQWs. The data in closed circles represent resonant excitation of the heavy-hole excitonic transition; data in open circles represent more energetic excitation with the specific pump photon energy specified in the captions. Solid lines indicate fits of the rise time with a Gaussian function convolved with an exponential decay (which is only apparent at longer pump-probe delays).

Table S1. Rise times of peak transient intersubband absorption signal

Sample (ML)	Pump Energy (eV)	Rise Time (fs)
4.5	3.26	188±56
4.5	2.42	80±25
5.5	3.10	317±38
5.5	2.25	116±30
6.5	2.95	464±142
6.5	2.15	127±54

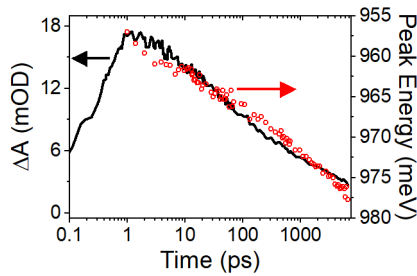


Figure S5. Raw transient absorption signal (left axis) of 5.5 ML CdSe CQW excited with an initial average exciton number of 3.5 per CQW. The peak energy of the induced absorption feature is shown in open red circles corresponding to the right-hand scale.

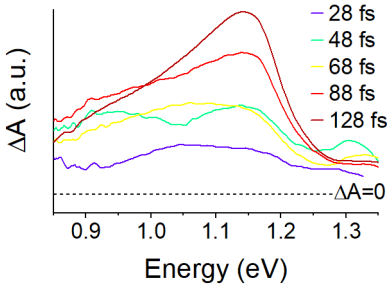


Figure S6. Transient spectra of intersubband absorption from 4.5 ML CdSe CQWs at pump-probe delay times of up to 128 fs. The non-monotonic curves are understood to indicate non-equilibrium distribution of electrons.

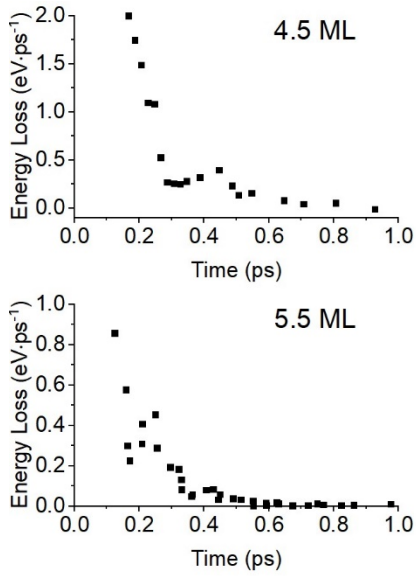


Figure S7. Energy loss rates of 4.5 ML and 5.5 ML CdSe CQWs based upon data of temperature estimates presented in Figures 3.

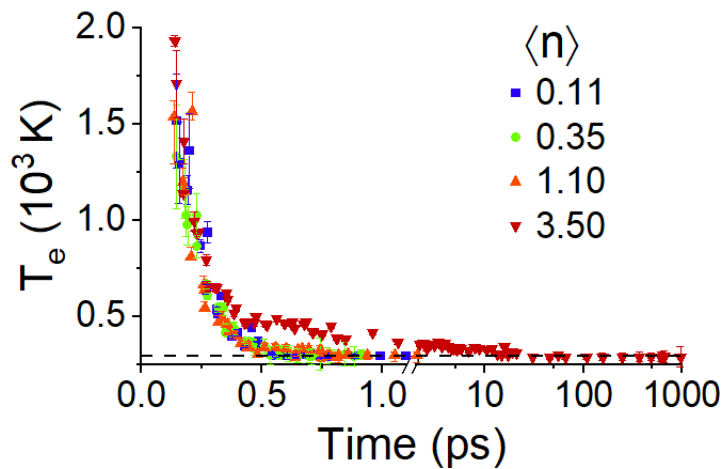


Figure S8. Linear y-axis scale plot of Figure 4. The dashed line indicates ambient temperature.

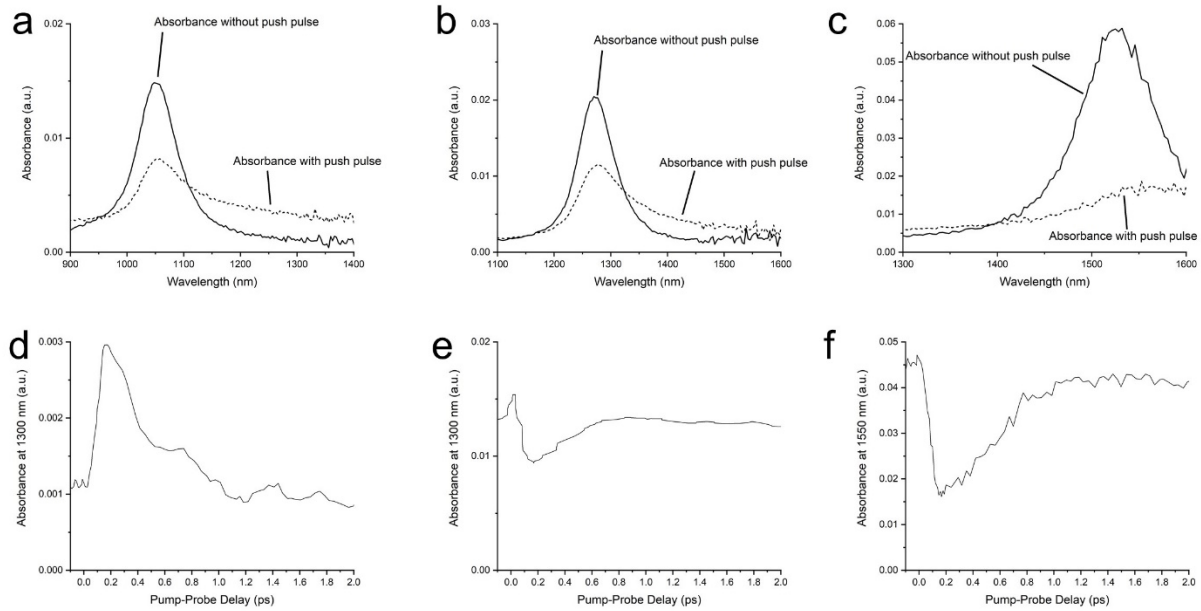


Figure S9. (a-c) Transient absorption spectra of (a) 4.5, (b) 5.5, and (c) 6.5 ML CdSe CQWs with and without a 0.41 eV push control pulse. (d-f) Line cuts of the same datasets at telecommunications wavelengths for the same (d) 4.5, (e) 5.5, and (f) 6.5 ML CdSe CQWs.

## References

- 1 P. von Allmen, M. Berz, G. Petrocelli, F.-K. Reinhart and G. Harbeke, *Semicond. Sci. Technol.*, 1988, **3**, 1211–1216.
- 2 G. Lasher and F. Stern, *Phys. Rev.*, 1964, **133**, A553–A563.
- 3 S. Ithurria, M. D. Tessier, B. Mahler, R. P. S. M. Lobo, B. Dubertret and A. L. Efros, *Nat. Mater.*, 2011, **10**, 936–941.
- 4 A. R. Greenwood, S. Mazzotti, D. J. Norris and G. Galli, *J. Phys. Chem. C*, 2021, acs.jpcc.0c10559.
- 5 A. S. Vengurlekar, S. S. Prabhu, S. K. Roy and J. Shah, *Phys. Rev. B*, 1994, **50**, 15461–15464.
- 6 S. S. Prabhu, A. S. Vengurlekar, S. K. Roy and J. Shah, *Phys. Rev. B*, 1995, **51**, 14233–14246.
- 7 Y. Yang, D. P. Ostrowski, R. M. France, K. Zhu, J. van de Lagemaat, J. M. Luther and M. C. Beard, *Nat. Photonics*, 2015, **10**, 53–59.
- 8 D. Zanato, N. Balkan, B. K. Ridley, G. Hill and W. J. Schaff, *Semicond. Sci. Technol.*, 2004, **19**, 1024–1028.
- 9 R. F. Leheny, J. Shah, R. L. Fork, C. V. Shank and A. Migus, *Solid State Commun.*, 1979, **31**, 809–813.
- 10 K. Kash and J. Shah, *Appl. Phys. Lett.*, 1984, **45**, 401–403.
- 11 M. Pelton, S. Ithurria, R. D. Schaller, D. S. Dolzhenkov and D. V. Talapin, *Nano Lett.*, 2012, **12**, 6158–6163.
- 12 G. Göbel, *Appl. Phys. Lett.*, 1974, **24**, 492–494.

- 13 R. F. Leheny and J. Shah, *Phys. Rev. Lett.*, 1977, **38**, 511–514.
- 14 C. V. Shank, R. L. Fork, R. F. Leheny and J. Shah, *Phys. Rev. Lett.*, 1979, **42**, 112–115.
- 15 J. F. Ryan, R. A. Taylor, A. J. Turberfield, A. Maciel, J. M. Worlock, A. C. Gossard and W. Wiegmann, *Phys. Rev. Lett.*, 1984, **53**, 1841–1844.
- 16 D. Von Der Linde and R. Lambrich, *Phys. Rev. Lett.*, 1979, **42**, 1090–1093.
- 17 M. H. Pilkuhn, *Phys. Status Solidi*, 1968, **25**, 9–62.
- 18 R. Terazzi, T. Gresch, M. Giovannini, N. Hoyler, N. Sekine and J. Faist, *Nat. Phys.*, 2007, **3**, 329–333.
- 19 H. Willenberg, G. H. Döhler and J. Faist, *Phys. Rev. B - Condens. Matter Mater. Phys.*, 2003, **67**, 1–10.
- 20 C. Ndebeka-Bandou, F. Carosella, R. Ferreira, A. Wacker and G. Bastard, *Appl. Phys. Lett.*, , DOI:10.1063/1.4766192.
- 21 C. Ndebeka-Bandou, F. Carosella, R. Ferreira and G. Bastard, *Appl. Phys. Lett.*, , DOI:10.1063/1.4804551.
- 22 F. Carosella, C. Ndebeka-Bandou, R. Ferreira, E. Dupont, K. Unterrainer, G. Strasser, A. Wacker and G. Bastard, *Phys. Rev. B - Condens. Matter Mater. Phys.*, 2012, **85**, 1–9.
- 23 O. Keller, A. Zayats and E. A. Vinogradov, *Adv. Mater. Opt. Electron.*, 1994, **4**, 417–421.
- 24 B. K. Ridley, *J. Phys. C Solid State Phys.*, 1982, **15**, 5899–5917.
- 25 J. Christen and D. Bimberg, *Phys. Rev. B*, 1990, **42**, 7213–7219.
- 26 Q. Li, Q. Liu, R. D. Schaller and T. Lian, *J. Phys. Chem. Lett.*, 2019, **10**, 1624–1632.
- 27 P. Geiregat, C. Rodá, I. Tanghe, S. Singh, A. Di Giacomo, D. Lebrun, G. Grimaldi, J. Maes, D. Van Thourhout, I. Moreels, A. J. Houtepen and Z. Hens, *Light Sci. Appl.*, , DOI:10.1038/s41377-021-00548-z.
- 28 S. Neeleshwar, C. C. L. Chen, C. B. Tsai, Y. Y. Chen, C. C. L. Chen, S. G. Shyu and M. S. Seehra, *Phys. Rev. B - Condens. Matter Mater. Phys.*, 2005, **71**, 6–9.
- 29 J. Shah, C. Lin, R. F. Leheny and A. E. DiGiovanni, *Solid State Commun.*, 1976, **18**, 487–489.



The submitted manuscript has been created by UChicago Argonne, LLC, Operator of Argonne National Laboratory (“Argonne”). Argonne, a U.S. Department of Energy Office of Science laboratory, is operated under Contract No. DE-AC02-06CH11357. The U.S. Government retains for itself, and others acting on its behalf, a paid-up nonexclusive, irrevocable worldwide license in said article to reproduce, prepare derivative works, distribute copies to the public, and perform publicly and display publicly, by or on behalf on the Government. The Department of Energy will provide public access to these results of federally sponsored research in accordance with the DOE Public Access Plan. <http://energy.gov/downloads/doe-public-access-plan>.